Research Article | Vol. 28, No. 24 / 23 November 2020 / Optics Express 35748
Optics EXPRESS

Analysis and suppression of the polarization error for the optical rotation detection system in an atomic comagnetometer

JIONG HUANG,[1] ZHUO WANG,[2,3,4,5,*] WENFENG FAN,[2] LI XING,[1] WEIJIA ZHANG,[1] LIHONG DUAN,[2] AND WEI QUAN[2,3,4,5]

[1] *School of Instrumentation Science and Opto-electronic Engineering, Beihang University, Beijing 100190, China*
[2] *Research Institute for Frontier Science, Beihang University, Beijing 100190, China*
[3] *Key Laboratory of Ministry of Industry and Information Technology on Quantum Sensing Technology, Beihang University, Beijing 100190, China*
[4] *Beijing Advanced Innovation Center for Big Data-Based Precision Medicine, Beihang University, Beijing 10019, China*
[5] *Beijing Academy of Quantum Information Sciences, Beijing 100193, China*
[*] *zhuowang@buaa.edu.cn*

Abstract: This paper investigates the laser polarization error in the optical rotation detection system (ORDS) of an atomic comagnetometer (ACM), which will seriously degrade the long-term performance of the ORDS. We first establish an optical transmission model of the ORDS by using Jones matrix concerning the optical imperfection of polarizers. Then, we analyze the polarization error based on this model and propose a novel error suppression method. Finally, we experimentally test the long-term performance of the ORDS and the ACM before and after the polarization error suppression to verify the effectiveness of the proposed method. The experimental results show that the long-term performance of the ORDS and the ACM can be improved by approximately 3.4 times with the proposed polarization error suppression method.

1. Introduction

The atomic comagnetometer studied in this paper is one kind of inertial measurement device that can measure the angular velocity of the carrier with ultra-sensitivity by means of hybrid atomic spin ensembles working in the spin-exchange relaxation-free (SERF) state. It can be used in fundamental physics research, such as tests of Lorentz and CPT violation [1,2] and searches for anomalous spin forces [3,4]. Furthermore, it also has a great potential to be made into a compact gyroscope for inertial navigation [5–7]. A rotation sensitivity of 2.1×10^{-8} rad s^{-1} Hz$^{-1/2}$ and a long-term stability on the order of 10^{-2} deg/h have been achieved based on the hybrid optical pumping K-Rb-^{21}Ne comagnetometer.

A typical atomic comagnetometer usually consists of four basic parts: the laser pumping system, the optical rotation detection system (ORDS), the magnetic shielding and compensation system, the vapor cell and its temperature control system. In particular, a high-stability ORDS is the basis of the high-stability inertial measurement capability of the ACM. However, there are various disturbances that degrade the stability of the ORDS. A typical disturbance is the low frequency fluctuation of laser polarization state, which not only seriously degrades the long-term stability of the ORDS [8–10], but also directly leads to the fluctuation of the ACM output signal in the form of a fictitious magnetic field (known as the light shift or AC Stark shift [11,12]). In this circumstance, the analysis and suppression of the polarization error is of great significance to improve the long-term performance of the ORDS.

The polarization error is common in optical measurement systems, such as the polarimeter, the fiber optic current sensor and the fiber optic gyroscope. On the one hand, a large number of

#406073 https://doi.org/10.1364/OE.406073
Journal © 2020 Received 24 Aug 2020; revised 15 Oct 2020; accepted 30 Oct 2020; published 10 Nov 2020

Optics EXPRESS

scholars have thoroughly studied the characteristics of the polarization error in these systems [10,13–16]. They concluded that the polarization error is mainly induced by the imperfection of the polarizer, which will cause Mach Zehnder interference in these optical measurement systems, resulting in laser phase coupling noise [15]. However, in the ORDS of the ACM, the situation is different. The polarization error will not only cause laser phase coupling noise, but also laser power splitting coupling error and fictitious magnetic field coupling error, which will eventually lead to low frequency drift of the detection signal. Unfortunately, the laser power splitting coupling error has not attracted enough attention in the ACM research field up to now, although it is a relatively large error term in practice. On the other hand, the polarization error suppression methods are also an important topic, which mainly include two categories: the direct suppression methods and the indirect compensation methods. The direct suppression methods always improve the extinction performance of the polarizer in a most straightforward way to suppress the polarization error [10]. However, the extinction performance of the polarizer cannot be infinitely improved, where the publicly reported smallest extinction ratio in the world is 2.9×10^{-10} and little progress has been made in the last 20 years [10,17]. Some scholars used the optical cavity as the polarizer to obtain the high extinction performance, which nevertheless is too complicated for the ACM [18]. In contrast, the indirect compensation methods based on the quarter wave plate have been developed to improve the measurement sensitivity of the null polarimetry [10], which however cannot suppress the laser power splitting coupling error in the ORDS and improve the long-term performance of the system.

In order to make up for the aforementioned weak applicability and deficiency of the existing polarization error suppression methods, and to improve the long-term performance of the ACM, we analyze the propagation characteristics and develop a novel suppression method of the polarization error in the ORDS in this paper. The analysis results reveal that the laser power control loop will cause laser polarization fluctuation, which in turn will lead to the laser power splitting error in the laser power control loop, and ultimately degrade the long-term performance of the system. This phenomenon was not reported in the researches on the ACM. The contribution of the proposed polarization error suppression method is that it can suppress the low-frequency long-term fluctuation in the ORDS. Besides, this error suppression method does not need additional optical components, and thus is not complicated to be applied to the ACM.

This paper is organized in the following way. Section II first establishes the optical transmission model of the ORDS by using Jones matrix, based on which, the propagation characteristics of the polarization error are studied. Then, the new polarization error suppression method is proposed according to the analysis results. Section III describes the experimental setup of the ACM and gives the basic experimental parameters. Section IV introduces the experimental operation steps of the proposed method in detail. The experimental results illustrate the effectiveness and practicability of the proposed polarization error suppression method. Finally, Section V draws the conclusion.

2. Analysis of the polarization error

The optical path diagram of the ORDS in the ACM is shown in the Fig. 1 [19,20]. The laser beam emitted from the laser source is purified to linearly polarized laser by the polarizer P1, and its vibration direction is defined as 0° direction. The half-wave plate before P1 is used to set the laser power emitted from the P1 by rotating the laser polarization direction. The linearly polarized laser becomes elliptically polarized after passing through the liquid crystal variable retarder (LCVR) with the fast axis along 45°direction. The polarizer P2 with the transmission axis along the 90° direction filters out the components of the elliptically polarized laser along the 0° direction to attenuate the laser power. The LCVR and two orthogonal polarizers constitute a variable optical attenuator (VOA), which is used as the actuator of the laser power stabilization system (LPSS). In order to further purify laser polarization state, a polarizing beam splitter (PBS)

Optics EXPRESS

instead of a non-polarizing beam splitter (NPBS) is used as the beam splitter. The half wave plate and the PBS before the cell form a continuous adjustable beam splitter to generate a feedback laser for the LPSS. The half wave plate and the PBS behind the cell constitute a polarimeter to measure the optical rotation angle produced by the cell.

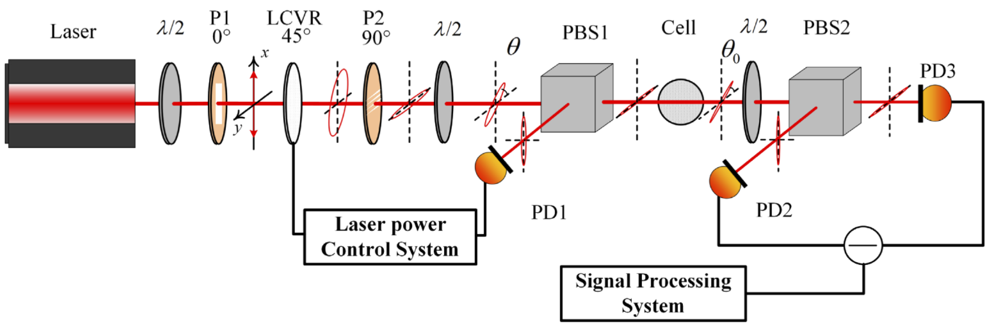

Fig. 1. Optical path diagram of optical rotation detection system in the atomic comagnetometer.

The mathematical model of laser polarization state evolution can be described by Jones matrix [21]. Define the 0 ° direction as the x-axis direction and the beam propagation direction as the z-axis direction. The Jones vector of the laser emitted from the laser source can be expressed as:

$$E_s = \begin{pmatrix} E_{sx} \\ E_{sy} \end{pmatrix}, \tag{1}$$

where E_{sx} and E_{sy} are the polarization components of the laser corresponding to x and y axes, respectively.

As has been said above, in the ORDS, polarizers play a key role in filtering the laser polarization component of the non-transmission axis and attenuating the laser power. In practice, however, the laser polarization component of the non-transparent axis usually cannot be completely filtered out due to the limited extinction performance of the real polarizer. The extinction performance of the real polarizer is affected not only by the material, but also by the laser incident angle. This imperfection of the polarizer that cannot completely stop the undesired polarization component can be described by the amplitude extinction ratio ε_p, which is defined as the ratio of the transmitted electric field when the polarizer transmission axis is perpendicular and parallel to the electric field direction, $\varepsilon_p = E_{\perp}^{trans}/E_{//}^{trans}$. In addition, the real polarizer also has the imperfection of birefringence, which also affects its extinction performance. Considering these two imperfect properties, the Jones matrix of a real polarizer transmitting along the x-axis can be expressed as [14,22]:

$$G_p = \begin{pmatrix} 1 & \gamma_p \\ \gamma_p & \varepsilon_p \end{pmatrix}. \tag{2}$$

Since the imperfect property γ_p is usually relatively small, in this study we ignore γ_p in the Jones matrix for simplicity. The Jones matrixes of the polarizers P1 and P2 in Fig. 1 can be written as follows:

$$G_{p1} = \begin{pmatrix} 1 & 0 \\ 0 & \varepsilon_p \end{pmatrix}, \tag{3}$$

Optics EXPRESS

$$G_{p2} = \begin{pmatrix} \varepsilon_p & 0 \\ 0 & 1 \end{pmatrix}. \tag{4}$$

The LCVR is a wave plate whose phase retardation can be changed continuously by the electro-optic birefringence of liquid crystal molecules. The relationship between the phase retardation and the effective AC driving voltage applied to the LCVR can be approximately described by the following equation [23]:

$$\delta(V) = \begin{cases} \delta_0 & (V \le V_c) \\ \delta_0 \left[\dfrac{2}{e^{-(\frac{V-V_c}{V_0})^M} + e^{(\frac{V-V_c}{V_0})^M}} \right]^2 & (V > V_c) \end{cases}, \tag{5}$$

where V_c is the threshold voltage at which the liquid crystal molecules begin to tilt, V_0 and M are constants corresponding to a specific LCVR. The Jones matrix of the LCVR with fast axis 45° to x axis is:

$$G_{LCVR} = \begin{pmatrix} \cos\left(\frac{\delta(V)}{2}\right) & -i\sin\left(\frac{\delta(V)}{2}\right) \\ -i\sin\left(\frac{\delta(V)}{2}\right) & \cos\left(\frac{\delta(V)}{2}\right) \end{pmatrix}. \tag{6}$$

then the Jones vector of the laser emitted from the polarizer P2 can be written as follows:

$$\begin{aligned} E_{oP2} &= G_{P2} \cdot G_{LCVR} \cdot G_{P1} \cdot E_s \\ &= \begin{pmatrix} \varepsilon_p E_{sx} \cos\left(\frac{\delta(V)}{2}\right) - i\varepsilon_p^2 E_{sy} \sin\left(\frac{\delta(V)}{2}\right) \\ \varepsilon_p E_{sy} \cos\left(\frac{\delta(V)}{2}\right) - iE_{sx} \sin\left(\frac{\delta(V)}{2}\right) \end{pmatrix}. \end{aligned} \tag{7}$$

For the convenience of analysis, suppose that the laser emitted by the laser source is a linearly polarized light along the x axis, ignore the polarization component E_{sy}, E_{oP2} can be simplified to:

$$E_{oP2} = \begin{pmatrix} \varepsilon_p E_{sx} \cos\left(\frac{\delta(V)}{2}\right) \\ -iE_{sx} \sin\left(\frac{\delta(V)}{2}\right) \end{pmatrix}. \tag{8}$$

It can be seen from the above formula that the laser emitted from the polarizer P2 is generally elliptically polarized due to the limited extinction ratio of the polarizer as long as the phase retardation $\delta(V)$ is not equal to π, and its ellipticity fluctuates with the phase retardation $\delta(V)$ (The ellipticity of polarized light (EOP)is defined as the ratio of the ellipse's minor to major axis [24]). The end motion equation of elliptically polarized light wave vibration vector can be expressed as ($\delta(V) \neq \pi$):

$$\frac{E_x^2}{\left(\varepsilon_p E_{sx} \cos\left(\frac{\delta(V)}{2}\right)\right)^2} + \frac{E_y^2}{\left(E_{sx} \sin\left(\frac{\delta(V)}{2}\right)\right)^2} = 1. \tag{9}$$

The polarization state of laser emitted from the polarizer P2 with different phase retardation is shown in Fig. 2.

The laser power splitting ratio of the PBS1 can be continuously changed by rotating the laser polarization direction θ angle through the half-wave plate in front of the PBS1. The Jones matrix

Optics EXPRESS

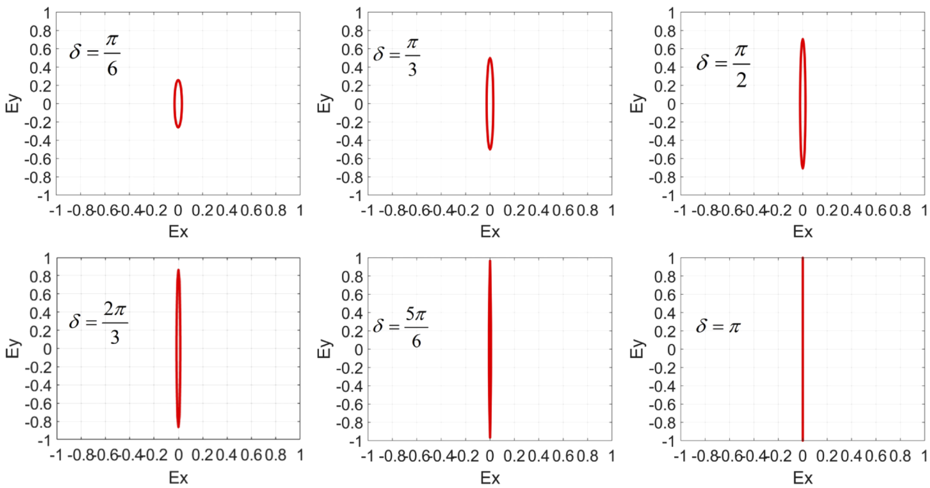

Fig. 2. The polarization state of laser emitted from the polarizer P2 with different phase retardation

of the half-wave plate can be described by:

$$G_{1/2\lambda} = \begin{pmatrix} \cos\theta & -\sin\theta \\ \sin\theta & \cos\theta \end{pmatrix}. \tag{10}$$

The transmitted direction and reflected direction of the PBS1 are equivalent to two polarizers, and the Extinction performance of the transmission direction is usually better than that of the reflection direction. Same as P1 and P2, their Jones matrixes can be written as follows:

$$G_{PBST} = \begin{pmatrix} 1 & 0 \\ 0 & \varepsilon_{pT} \end{pmatrix}, \tag{11}$$

$$G_{PBSF} = \begin{pmatrix} \varepsilon_{pF} & 0 \\ 0 & 1 \end{pmatrix}. \tag{12}$$

ε_{pT} and ε_{pF} are the amplitude extinction ratio of transmitted direction and reflected direction, respectively. Then we can derive the Jones vectors of the transmitted and reflected laser:

$$\begin{aligned} E_T &= G_{PBST} \cdot G_{1/2\lambda} \cdot E_{oP2} = \\ &= E_{sx} \begin{pmatrix} \varepsilon_p \cos\left(\frac{\delta(V)}{2}\right)\cos\theta + i\sin\left(\frac{\delta(V)}{2}\right)\sin\theta \\ \varepsilon_p\varepsilon_{pT}\cos\left(\frac{\delta(V)}{2}\right)\sin\theta - i\varepsilon_{pT}\sin\left(\frac{\delta(V)}{2}\right)\cos\theta \end{pmatrix}, \end{aligned} \tag{13}$$

$$\begin{aligned} E_F &= G_{PBSF} \cdot G_{1/2} \cdot E_{oP2} = \\ &= E_{sx} \begin{pmatrix} \varepsilon_{pF}\varepsilon_p \cos\left(\frac{\delta(V)}{2}\right)\cos\theta + i\varepsilon_{pF}\sin\left(\frac{\delta(V)}{2}\right)\sin\theta \\ \varepsilon_p\cos\left(\frac{\delta(V)}{2}\right)\sin\theta - i\sin\left(\frac{\delta(V)}{2}\right)\cos\theta \end{pmatrix}. \end{aligned} \tag{14}$$

And then the power of the transmitted and reflected laser could be deduced according to their Jones vectors:

$$
\begin{aligned}
P_T &= |\tilde{E}_{Tx}|^2 + |\tilde{E}_{Ty}|^2 \\
&= E_{sx}^2(\varepsilon_p^2\cos^2\theta + \varepsilon_{pT}^2\varepsilon_p^2\sin^2\theta)\cos^2\left(\frac{\delta(V)}{2}\right) \\
&+ E_{sx}^2(\sin^2\theta + \varepsilon_{pT}^2\cos^2\theta)\sin^2\left(\frac{\delta(V)}{2}\right),
\end{aligned}
\tag{15}
$$

$$
\begin{aligned}
P_F &= |\tilde{E}_{Fx}|^2 + |\tilde{E}_{Fy}|^2 \\
&= E_{sx}^2(\varepsilon_{pF}^2\varepsilon_p^2\cos^2\theta + \varepsilon_p^2\sin^2\theta)\cos^2\left(\frac{\delta(V)}{2}\right) \\
&+ E_{sx}^2(\varepsilon_{pF}^2\sin^2\theta + \cos^2\theta)\sin^2\left(\frac{\delta(V)}{2}\right).
\end{aligned}
\tag{16}
$$

The transmitted laser is used to detect the optical rotation angle of the cell, while the reflected laser is used for the LPSS to stabilize the laser power. Suppose that the half-wave plate behind the cell rotates the laser polarization direction by 45 degrees, which means that the polarimeter is in balance when the optical rotation angle of the cell is zero. Ignore the laser absorption effect of the cell, the output of ORDS could be expressed as [25]:

$$U = P_T\cos^2\left(\theta_o - \frac{\pi}{4}\right) - P_T\sin^2\left(\theta_o - \frac{\pi}{4}\right). \tag{17}$$

Equations (8) to (17) reveal the basic propagation path of the polarization error in the ODRS: firstly, during the LPSS working, the change of the LCVR phase retardation causes random fluctuation of the laser polarization state, which will lead to the inconsistency of power fluctuation between transmitted and reflected laser. Then this inconsistency will in turn lead to the laser power control error of the LPSS, resulting in the transmitted laser power fluctuation. Finally, the transmitted laser power fluctuation will be coupled to the output of the ORDS and bring about the bias drift as long as the optical rotation angle θ_o is not zero. This kind of polarization error is called laser power splitting coupling error in this paper. In order to further figure out the variation law of this error, we define the laser power splitting ratio of the PBS1 as the ratio of the transmitted laser power to the reflected laser power. Then it can be expressed as:

$$\alpha(\theta, \delta(V)) = \frac{P_T}{P_F}. \tag{18}$$

By taking the partial derivative of the above equation with respect to $\delta(V)$ and making the partial derivative to zero, two solutions can be obtained:

$$\theta = \frac{\pi}{4}, \quad \text{and} \quad \delta(V) = \pi. \tag{19}$$

The above result indicates that there is an optimization point where the laser power splitting ratio α does not fluctuate with the LCVR phase retardation $\delta(V)$. This means that the laser power splitting ratio is not sensitive to the laser polarization fluctuation caused by the laser power control loop. Therefore, the laser power splitting coupling error can be well suppressed at this optimized point.

The above analysis results are verified by the simulation of Eq. (18). The simulation results are shown in Fig. 3 and Fig. 4. Figure 3 shows the variation curve of laser power splitting ratio α with the control voltage of the LCVR under different ε_p conditions. It can be seen from the figure that the smaller the ε_p (the better the extinction performance of the polarizer), the smaller the relative variation of the splitting ratio with the phase retardation. Therefore, the improvement of the extinction performance of the polarizer is an effective method to suppress the laser power coupling polarization error. In addition, this curve has a pole at the control voltage whose phase retardation is π, which is consistent with the solution of Eq. (19). Figure 4 shows the relative variation curve of beam splitting ratio α with θ under different ε_p conditions. The change of θ from 0° to 90° is the same as the change of α from 0 to infinity. It can be seen from the figure that this curve has a pole at $\theta = \pi/4$, which is also consistent with the previous theoretical analysis. This means that the polarization error could be further suppressed by optimizing the splitting ratio of the PBS through the half wave plate. This indirect compensation polarization error suppression method based on the half wave plate will be introduced in detail in Section IV.

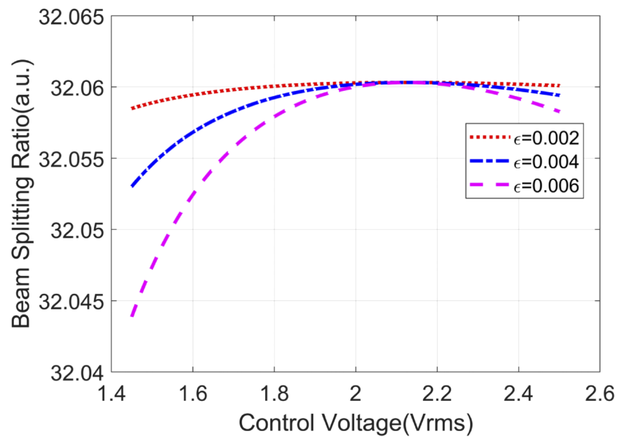

Fig. 3. Variation curve of beam splitting ratio α with the control voltage of the LCVR under different ε_p conditions.

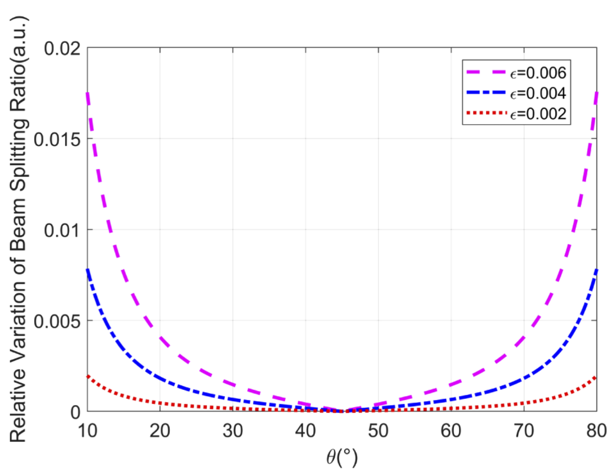

Fig. 4. Relative variation curve of beam splitting ratio α with θ under different ε_p conditions.

3. Experimental setup

In order to verify the theoretical analysis and simulation results in Section II, the experiment is performed in the compact K-Rb-^{21}Ne ACM, which is shown in Fig. 5. The whole system is composed of four parts, which are laser pumping system, laser detection system, magnetic

Optics EXPRESS

shielding and magnetic compensation system, the vapor cell and its temperature control system [5,26,27]. Laser pumping and detection systems are used to polarize and detect atomic spins, respectively. Temperature control system and magnetic shielding and magnetic compensation system provide a high temperature and weak magnetic environment for the vapor cell, respectively. In this environment, the spin exchange relaxation of alkali metal atoms can be greatly suppressed, which is conducive to improving the signal-to-noise ratio of the system [28,29].

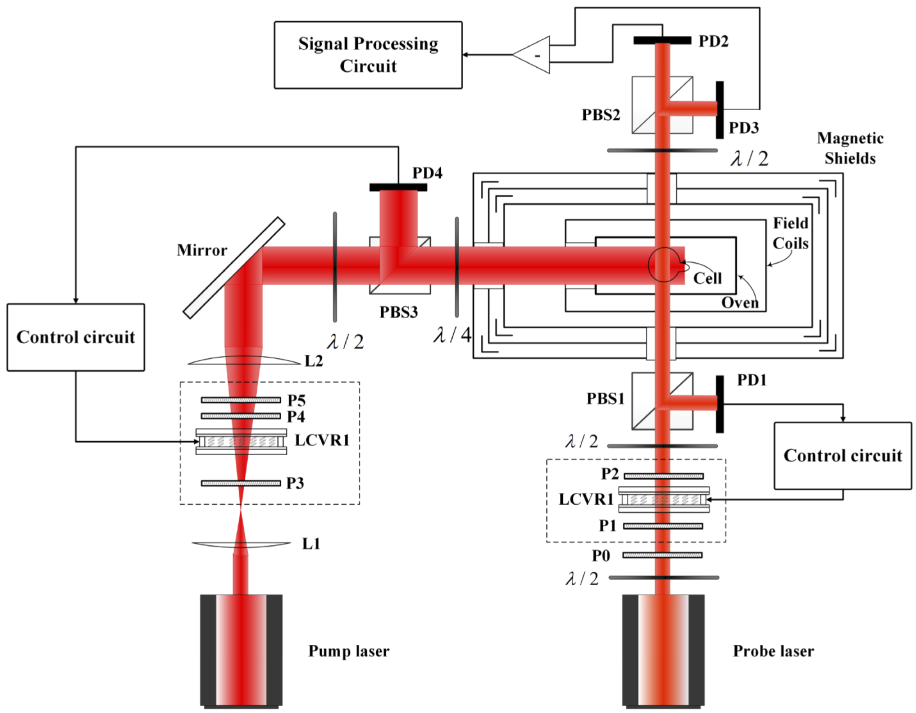

Fig. 5. Schematic diagram of a basic atomic comagnetometer with the laser power stabilization system.

In the experiment, a 10 mm diameter spherical vapor cell containing a mixture of K and Rb alkali metals, 50 torr of N_2 gas and 3 amagat of ^{21}Ne gas, is used. The cell is heated to 185°C by a boron nitride ceramic oven with a 100KHz alternating current heater. The atomic number density ratio of K to Rb at this operating temperature is approximately 1:85. The pump beam is generated by a distributed Bragg reflector (DBR) laser device with a central frequency of 770.108nm (K D1 resonance line) and an output power of 80 mW. The spot diameter of the pump beam is expanded to 10 mm by two planoconvex lenses L1 and L2. The probe beam is generated a distributed feedback (DFB) laser device with a central frequency of 795.311nm (About 0.3nm to the blue side of the Rb D1 resonance line) and an output power of 40 mW. The polarizing beam splitters PBS1 and PBS3 in front of the vapor cell play the role of the polarizer and beam splitter at the same time. The PBS2 and the half-wave plate constitute a polarimeter to analyze the polarization of the transmitted probe laser [25]. The power of the output beams from the polarimeter is detected by the balanced photodetector composed of the photodiodes PD2 and PD3. The power fluctuations of the pumping laser and the detection laser are suppressed by the LCVR LPSS. The polarizer P0 and the half-wave plate before P0 are used to change the incident laser power of the ORDS. The photodiode PD2 is also used to evaluate the stability of detection laser power by removing PBS2.

Optics EXPRESS

4. Suppression method and experimental verification

According to the analysis in Section II, the laser power splitting coupling error caused by laser polarization fluctuation could be suppressed by looking for the insensitive point where the laser power splitting ratio does not fluctuate with the laser polarization through rotating the half wave plate before PBS1. Theoretically, this insensitive point is the point where the laser power splitting ratio is equal to 1:1. However, in practice, there are some deviations between the theory and the practice, because only the imperfect characteristics of the polarizer which have the greatest influence on the system are considered in the process of theoretical modeling. The imperfections also exist in other optical components including half-wave plate and LCVR, and there are some alignment errors in the optical path. Therefore, this insensitive point needs to be obtained by the experiment in practice. The operation steps of the experimental method for finding this insensitive point proposed in this paper are as follows: firstly, lock the reflected laser power of the PBS1 to a constant value by the LCVR LPSS. Then change the incident laser power of the LCVR LPSS by rotating the half-wave plate before P0. For the LCVR LPSS, the change of incident laser power is equivalent to an active disturbance excitation signal. This system will maintain the reflected laser power to the constant value before the disturbance by adjusting the attenuation of the LCVR VOA. Finally, the polarization error can be obtained by measuring the output variation of the ORDS. The output variation with the disturbance can be adjusted to near zero level by rotating half-wave plate in front of the PBS1, and the splitting ratio at this time is the best one to suppress the polarization error. Figure 6 shows the variation curve of the ODRS output signal with the LCVR control voltage during the above operation process.

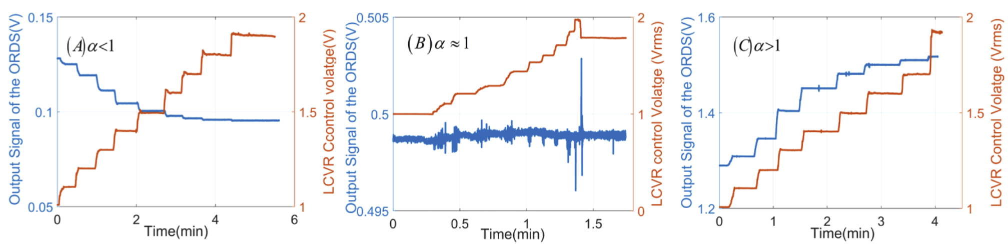

Fig. 6. The variation curve of the ODRS output signal with the LCVR control voltage: (A) $\alpha<1$, (B) $\alpha \approx 1$, (C) $\alpha>1$.

The relative variation curve of the ORDS output signal versus the LCVR control voltage measured by the above method based on the experimental setup is shown in Fig. 7. The test points in Fig. 7 represent the difference of the ORDS output signal under different control voltages relative to that under the control voltage of 1V. It can be seen from the figure that the experimental curve is consistent with the theoretical curve presented in the section II. When the laser power splitting ratio is close to 0.9982, the output signal of ODRs is insensitive to the change of LCVR control voltage, which means that the laser power splitting error caused by laser polarization fluctuation has been well suppressed.

The long-term stability of the detection laser power locked by the LCVR LPSS before and after polarization error (PE) suppression is tested under the same ambient temperature (The ambient temperature fluctuation is controlled within 1°C through the laboratory air conditioner). The test time is three hours and the sampling frequency is 200Hz. The long-term stability of the transmitted laser power is evaluated by the relative Allan variance [30]. The experimental results are shown in Fig. 8. As can be seen from the curve (1)–(3) in the figure, the long-term stability (After 10 seconds of cluster time) of the laser power after being locked by the LCVR LPSS can be improved by nearly two orders of magnitude. After suppressing the polarization error by the method proposed in this paper, the long-term stability at 100s of laser power can be improved by

Optics EXPRESS

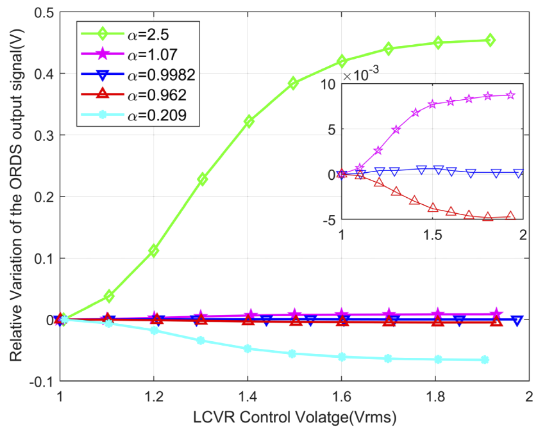

Fig. 7. Curve of the relative variation curve of the ORDS output signal versus the control voltage of the LCVR

nearly 5 times and the long-term trend term (After 100 seconds of cluster time) can be greatly suppressed.

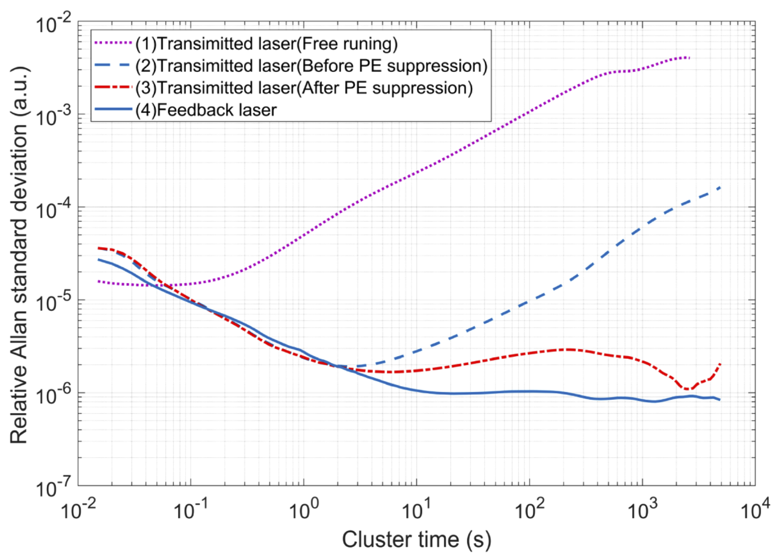

Fig. 8. The relative Allan variance of the detection laser power. (1) Laser power Free-running, (2) Laser power locked before the PE suppression, (3) Laser power locked after the PE suppression, (4) Feedback laser power.

The long-term performance of the ORDS and the ACM is also tested before and after the PE suppression. The test time is three hours and the sampling frequency is 200Hz. The detection laser power entering the vaper cell is 1mW and the pump laser power is 40mW. Due to insufficient pump power, the beam splitting ratio of the pump laser is set to 20:1. The polarization error of laser pumping system is suppressed by using two GT polarizers after the LCVR. The experimental results are shown in Fig. 9. It can be seen from the figure that the short-term stability (random walk) of the ORDS system before 1s remains basically unchanged before and after the polarization error suppression, while that of the ACM before 10s remains unchanged. However, it is obvious that the long-term stability of the ORDS after 1 s and that of the ACM after 10 s can be well improved after PE suppression, which verifies the effectiveness of the proposed PE suppression method to improve the long-term performance of the system. The long-term stability at 100s of the ORDS and the ACM can be improved by approximately 3.4 times.

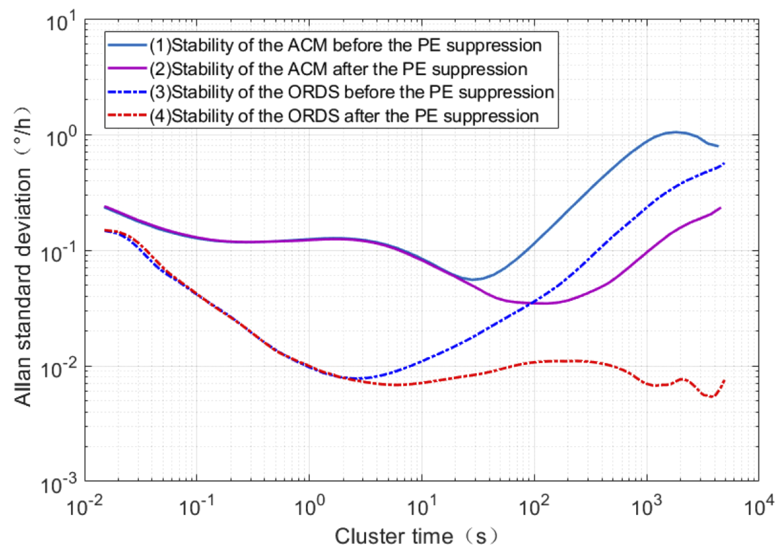

Fig. 9. Allan standard deviation curve of the ORDS and the ACM. (1) Stability of the ACM before the PE suppression, (2) Stability of the ACM after the PE suppression, (3) Stability of the ORDS before the PE suppression, (4) Stability of the ORDS after the PE suppression.

In order to more intuitively verify the effectiveness of the proposed PE suppression method, the 6-hour synchronous time-domain variation curve of the detection signal and the LCVR control voltage before and after PE suppression is shown in Fig. 10. It can be seen from the figure that before the PE suppression, there is a strong negative correlation between the detection signal and the LCVR control voltage and a large trend term error in the detection signal. However, after the PE suppression, the correlation between the detection signal and the LCVR control voltage is greatly weakened, and the low frequency drift of the detection signal is well suppressed.

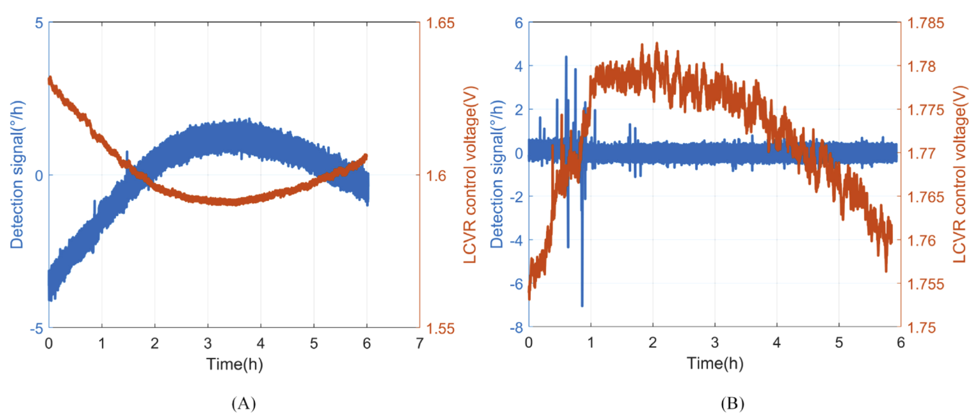

Fig. 10. Variation curve of the detection signal with the LCVR control voltage. (A) Before the PE suppression, (B) After the PE suppression

Optics EXPRESS

5. Conclusion

In conclusion, we have established an optical transmission model of the ORDS concerning the optical imperfection of the polarizers by using Jones matrix and analyzed the propagation characteristics of the polarization error based on this model. The theoretical analysis shows that the change of the LCVR phase retardation during the LPSS working will induce polarization state randomly coupling, and will express laser power splitting coupling error in the ORDS due to the imperfection of polarizers. This error will be coupled to the ORDS output and seriously degrade the long-term performance of the ACM. This propagation property of the polarization error in the ORDS have not attracted enough attention in the ACM research field up to now. In order to suppress this error, a new indirect compensation method based on the half-wave plate is proposed and the effectiveness of this method is verified by experiment. The experimental results show that the long-term stability of the detection laser power can be improved by nearly 5 times after suppressing this error by using the proposed method. Correspondingly, the long-term performance of the ORDS and the ACM can be improved by approximately 3.4 times. The effect of the polarization error suppression could be further improved by reducing the alignment errors of the optical path. The analysis results and the error suppression method presented here can lay a theoretical and experimental foundation for the design of the ORDS, and will be significant for optimizing the long-term performance of the high precision ACM.

Funding

Beijing Academy of Quantum Information Sciences (Y18G34); National Key Research and Development Program of China (2016YFB0501600, 2017YFB0503100); National Natural Science Foundation of China (61673041, 61721091, 61773043).

Disclosures

The authors declare that there are no conflicts of interest related to this article.

References

1. J. Brown, S. Smullin, T. Kornack, and M. Romalis, “New limit on lorentz-and CPT-violating neutron spin interactions,” Phys. Rev. Lett. **105**(15), 151604 (2010).
2. M. Smiciklas, J. Brown, L. Cheuk, S. Smullin, and M. Romalis, “New Test of Local Lorentz Invariance Using a 21Ne-Rb-K Comagnetometer,” Phys. Rev. Lett. **107**(17), 171604 (2011).
3. G. Vasilakis, J. M. Brown, T. W. Kornack, and M. V. Romalis, “Limits on New Long Range Nuclear Spin-Dependent Forces Set with a K-3He Comagnetometer,” Phys. Rev. Lett. **103**(26), 261801 (2009).
4. K. Tullney, F. Allmendinger, M. Burghoff, W. Heil, S. Karpuk, W. Kilian, S. Knappe-Grüneberg, W. Müller, U. Schmidt, A. Schnabel, F. Seifert, Y. Sobolev, and L. Trahms, “Constraints on Spin-Dependent Short-Range Interaction between Nucleons,” Phys. Rev. Lett. **111**(10), 100801 (2013).
5. T. W. Kornack, R. K. Ghosh, and M. V. Romalis, “Nuclear Spin Gyroscope Based on an Atomic Comagnetometer,” Phys. Rev. Lett. **95**(23), 230801 (2005).
6. F. Wenfeng, Q. Wei, L. Feng, D. Lihong, and L. Gang, “Low drift nuclear spin gyroscope with probe light intensity error suppression,” Chin. Phys. B **28**(11), 110701 (2019).
7. R. Li, W. Fan, L. Jiang, L. Duan, W. Quan, and J. Fang, “Rotation sensing using a K-Rb-21Ne comagnetometer,” Phys. Rev. A **94**(3), 032109 (2016).
8. L. Jiang, W. Quan, R. Li, W. Fan, F. Liu, J. Qin, S. Wan, and J. Fang, “A parametrically modulated dual-axis atomic spin gyroscope,” Appl. Phys. Lett. **112**(5), 054103 (2018).
9. S. Feng and O. Pfister, “Sub-shot-noise heterodyne polarimetry,” Opt. Lett. **29**(23), 2800–2802 (2004).
10. D. He, B. Xie, and S. Feng, “Null polarimetry near shot noise limit at 1 Hz,” Rev. Sci. Instrum. **87**(4), 043102 (2016).
11. B. S. Mathur, H. Tang, and W. Happer, “Light Shifts in the Alkali Atoms,” Phys. Rev. **171**(1), 11–19 (1968).
12. S. P. Krzyzewski, A. R. Perry, V. Gerginov, and S. Knappe, “Characterization of noise sources in a microfabricated single-beam zero-field optically-pumped magnetometer,” J. Appl. Phys. **126**(4), 044504 (2019).
13. C. Laskoskie, B. Szafraniec, and W. Trammell, *Depolarized interferometer fiber optic gyro with improved polarization error suppression*, Fibers ‘92 (SPIE, 1993), Vol. 1795.
14. L. Wang, J. Ji, Q. Bo, Y. Yuan, and J. Qian, “Modeling and simulation of polarization errors in Sagnac fiber optic current sensor,” Optik **125**(17), 4770–4775 (2014).

Optics EXPRESS

15. J. N. Chamoun and M. J. F. Digonnet, "Noise and Bias Error Due to Polarization Coupling in a Fiber Optic Gyroscope," J. Lightwave Technol. **33**(13), 2839–2847 (2015).
16. G. Xin, J. Zhu, C. Luo, J. Tang, W. Li, Y. Cao, and H. Xu, "Polarization Error Analysis of an All-Optical Fibre Small Current Sensor for Partial Discharge," J. Electr. Eng. Technol. **15**(5), 2199–2210 (2020).
17. Y. Takubo, N. Takeda, J. H. Huang, K. Muroo, and M. Yamamoto, "Precise measurement of the extinction ratio of a polarization analyser," Meas. Sci. Technol. **9**(1), 20–23 (1998).
18. S. Saraf, R. L. Byer, and P. J. King, "High-extinction-ratio resonant cavity polarizer for quantum-optics measurements," Appl. Opt. **46**(18), 3850–3855 (2007).
19. L. Jiang, W. Quan, Y. Liang, J. Liu, L. Duan, and J. Fang, "Effects of pump laser power density on the hybrid optically pumped comagnetometer for rotation sensing," Opt. Express **27**(20), 27420–27430 (2019).
20. L. Xing, Y. Zhai, W. Fan, J. Huang, T. Song, W. Ye, and W. Quan, "Miniaturized optical rotation detection system based on liquid crystal variable retarder in a K-Rb-21Ne gyroscope," Opt. Express **27**(26), 38061–38070 (2019).
21. E. Hecht, *Optics* (Pearson Education, Incorporated, 2017).
22. W. K. Burns, P. F. Liao, and P. Kelley, Optical fiber rotation sensing (Academic University, 2012).
23. Q. Liang, L. Chen, G. Lei, W. Wu, and B. Zhou, *Laser intensity stabilization with a liquid crystal variable retarder for a nuclear magnetic resonance gyroscope prototype*, Applied Optics and Photonics China (AOPC2015) (SPIE, 2015), Vol. 9671.
24. J. Volakis, R. C. Johnson, and H. Jasik, *Antenna Engineering Handbook*, 4th Edition (McGraw-Hill Education, 2007).
25. R. Jiménez-Martínez, S. Knappe, W. C. Griffith, and J. Kitching, "Conversion of laser-frequency noise to optical-rotation noise in cesium vapor," Opt. Lett. **34**(16), 2519–2521 (2009).
26. F. Coils, P. Beam, P. Cell, and D. Laser, "Nuclear-Spin Gyroscope Based on an Atomic Co-Magnetometer," Phys. Rev. Lett. **95**(23), 230801 (2005).
27. R. Li, "Rotation sensing using a K-Rb-Ne21 comagnetometer," (2016).
28. W. Happer and A. C. Tam, "Effect of Rapid Spin Exchange on the Magnetic-Resonance Spectrum of Alkali Vapors," Phys. Rev. A **16**(5), 1877–1891 (1977).
29. J. C. Allred, R. N. Lyman, T. W. Kornack, and M. V. Romalis, "High-sensitivity atomic magnetometer unaffected by spin-exchange relaxation," Phys. Rev. Lett. **89**(13), 130801 (2002).
30. F. Tricot, D. H. Phung, M. Lours, S. Guérandel, and E. D. Clercq, "Power stabilization of a diode laser with an acousto-optic modulator," Rev. Sci. Instrum. **89**(11), 113112 (2018).